

# Varying organic content in fish otoliths: Effects on SIMS-based $\delta^{18}\text{O}$ measurements and possible corrections

Timo D. Rittweg<sup>a,b,\*</sup>, Michael Wiedenbeck<sup>c</sup>, Jan Fietzke<sup>d</sup>, Clive Trueman<sup>e</sup>

<sup>a</sup> Leibniz Institute of Freshwater Ecology and Inland Fisheries (IGB), Müggelseedamm 310, Berlin 12587, Germany

<sup>b</sup> Division of Integrative Fisheries Management, Faculty of Life Sciences, Humboldt-Universität zu Berlin, Unter den Linden 6, Berlin 10099, Germany

<sup>c</sup> German Research Center for Geosciences (GFZ) Potsdam, Telegrafenberg, Potsdam 14473, Germany

<sup>d</sup> GEOMAR Helmholtz Center for Ocean Research Kiel, Wischhofstr. 1-3, Kiel 24148, Germany

<sup>e</sup> School of Ocean and Earth Science, University of Southampton Waterfront Campus, European Way, Southampton SO143ZH, UK

## ARTICLE INFO

### Keywords:

Thermometry  
Isotope ecology  
Biogenic carbonates  
Ontogeny  
Growth

## ABSTRACT

Varying organic contents in otoliths have complex and sometimes counterintuitive effects on intra-otolith  $\delta^{18}\text{O}$  measurements. This is often addressed by roasting otoliths or applying fixed corrections, however, the underlying chemical and physiological mechanisms involved are poorly understood and have not been tested in a quantitative manner, potentially rendering such corrections unreliable. Using high-resolution secondary ion mass spectrometry (SIMS) measurements of  $\delta^{18}\text{O}$  values paired with  $\text{OH}/^{16}\text{O}$  ion ratios as organic proxy, we derived quantitative relationships of these measurements over the entire life of a large sample of northern pike (*Esox lucius*) otoliths from freshwater and brackish habitats. We assessed  $\text{OH}/^{16}\text{O}$  ion count ratio as an organic tracer, and estimated its relationship with  $\delta^{18}\text{O}$  determinations. We developed a pointwise correction approach that accounted for variations in otolith organic contents.  $\text{OH}/^{16}\text{O}$  ion ratio profiles agreed with other organic proxies, confirming them as reliable tracer of organic content. We detected an inverse relationship between  $\delta^{18}\text{O}$  values and  $\text{OH}/^{16}\text{O}$  ion ratio, with elevated  $\text{OH}/^{16}\text{O}$  ion ratios near otolith cores.  $\text{OH}/^{16}\text{O}$  ratios decreased with distance to the core. Pairwise corrections for the effect of  $\text{OH}/^{16}\text{O}$  ratios on  $\delta^{18}\text{O}$  values resulted in a mean offset between uncorrected and corrected values of 0.52 ‰, suggesting an approximately 2 °C bias towards warmer temperature if uncorrected data were to be used for  $\delta^{18}\text{O}$  thermometry. Simultaneous determination on organic- and inorganic-bound oxygen resulted in a negative offset of  $\delta^{18}\text{O}$ , which varies with the life history of individual fish. Varying offsets in  $\delta^{18}\text{O}$  values within individual life histories could be accounted for using our correction. We recommend future SIMS-based  $\delta^{18}\text{O}$  thermometry studies to estimate the local organic content to assess whether correction is warranted. We further offer more general recommendations on how future studies may assess whether corrections for organics are necessary.

## 1. Introduction

Otoliths record time-resolved chemical signals from the ambient water, enabling inferences on environmental factors throughout the individual animal's life history (Reis-Santos et al., 2022). Otolith elemental composition reflects environmental as well as physiological conditions, aiding in understanding physiological processes, migration, and population connectivity (Campana and Thorrold, 2001; Heidemann et al., 2012; Kafemann et al., 2000; Chung et al., 2020). For instance, intraotolith  $\delta^{18}\text{O}$  determinations are commonly used to reconstruct past water temperatures in fishes (Patterson et al., 1993) and to track large-scale migrations and habitat shifts (Darnaude and Hunter, 2018).

However, the chemical composition of otoliths can be influenced by multiple physiological factors, which need to be understood (Campana and Thorrold, 2001).

Otoliths are composed mainly of crystalline calcium carbonate precipitated from endolymphatic fluid within the inner ear of fishes (Stevenson and Campana, 1992). Precipitation is facilitated by an organic scaffolding of largely acidic glycoproteins (Degens, 1969). During otolith growth, minor and trace elements within the endolymph are incorporated into the otolith by replacing calcium ions in the crystal lattice, adsorption to surfaces, binding to the organic matrix, or incorporation in interstitial spaces between calcium carbonate crystals (Campana, 1999). In temperate fishes, organic matter concentrations

\* Corresponding author at: Leibniz Institute of Freshwater Ecology and Inland Fisheries (IGB), Müggelseedamm 310, Berlin 12587, Germany.

E-mail address: [timo.rittweg@igb-berlin.de](mailto:timo.rittweg@igb-berlin.de) (T.D. Rittweg).

<https://doi.org/10.1016/j.fishres.2024.107239>

Received 26 July 2024; Received in revised form 8 November 2024; Accepted 25 November 2024

Available online 24 December 2024

0165-7836/© 2024 The Authors. Published by Elsevier B.V. This is an open access article under the CC BY license (<http://creativecommons.org/licenses/by/4.0/>).

fluctuate seasonally, influencing light absorption (organic matter has a higher absorption than carbonate), resulting in visually discernible growth zones (Campana, 1999; Stevenson and Campana, 1992). Fast growth, which in temperate fishes often takes place in summer, leads to higher organic matter content, yielding opaque zones, while slower growth, which often occurs in winter for temperate fishes, produces more translucent zones due to higher proportion of calcium carbonate (Stevenson and Campana, 1992). Critically, otoliths, like many biomineralized tissues, are composite materials. For example, intra-otolith  $\delta^{18}\text{O}$  values are commonly assumed to reflect only oxygen bound within the calcium carbonate. However, the glycoprotein-rich organic matter, which constitutes between 0.2% and 10% of total otolith mass (Degens et al., 1969), also contains oxygen in form of hydroxy groups. Measurements of  $\delta^{18}\text{O}$  in otoliths may therefore be biased by admixing organic and mineral phases (Degens et al., 1969; Guiguer et al., 2003; Hane et al., 2020, 2022).

The impact of oxygen release from organic matter and calcium carbonate on  $\delta^{18}\text{O}$  values in otoliths has been first noted by Guiguer et al. (2003) and Matta et al. (2013). Removal of organic phases by roasting (Guiguer et al., 2003) resulted in significantly higher  $\delta^{18}\text{O}$  values as compared to unroasted samples, implying preferential removal of a phase depleted in  $^{18}\text{O}$ . Similarly, Matta et al. (2013) observed a roughly 1‰ increase for roasted (360 °C for 3.5 h under vacuum) vs. unroasted halves of a yellow sole (*Limanda aspera*). The studies used different analytical methods (acid digestion followed by continuous flow IRMS and SIMS, respectively), but reported similar effects on  $\delta^{18}\text{O}$  values, likely resulting from the presence of organics. The effect of mixed organic-anorganic matter on isotope measurements was also described more generally by Oehlerich et al. (2013), and therefore seems to be independent of measurement method. More recent research on otoliths (Hane et al., 2020; Helser et al., 2018; Wycech et al., 2018) also found consistent offsets between untreated and roasted otoliths using SIMS and acid digestion. Observed offset were hypothesized to result from organic matter, differences between sample and reference materials, or from water adsorption. Although such offsets appear to be common across species and systems, the underlying mechanism(s) remains unclear.

Reported effects of organic matter on  $\delta^{18}\text{O}$  values prompted some studies to roast otoliths to reduce or eliminate the organic contents (e.g., Burbank et al., 2020; Geffen, 2012). However, roasting has led to inconsistent outcomes (Guiguer et al., 2003), and questions persist regarding potential heat-induced phase transitions (e.g., aragonite to calcite) in the carbonate matrix (Matta et al., 2013). Other studies, such as Hane et al. (2022) and Morissette et al. (2020), applied mathematical corrections to  $\delta^{18}\text{O}$  measurements (+0.41‰ and +1‰ shifts, respectively), but applying such general correction factors across all measurements likely overlooks individual ontogenetic effects and habitat shifts (von Bertalanffy, 1938; Werner, 1988). To understand how individual life history influences intraotolith organic content and  $\delta^{18}\text{O}$  values, quantification of organics in otoliths are needed. Contributions of hydroxy groups,  $\text{OH}^-$ , to the overall oxygen content can be measured during SIMS  $\delta^{18}\text{O}$  determinations by using a multi-collection strategy measuring both the  $^{18}\text{O}/^{16}\text{O}$  and the  $\text{OH}/^{16}\text{O}$  ratios of the emitted secondary ions. This offers a potential proxy for organic content, as oxygen in organic matter glycoproteins can be expected to be primarily bound as hydroxy groups (Degens et al., 1969). Validated by established organic proxies, such as phosphorus and sulfur concentrations,  $\text{OH}/^{16}\text{O}$  ratio might be a promising tool for quantifying the intraotolith organic matter distributions.

Our study assessed the impact of intraotolith organics on  $\delta^{18}\text{O}$  measurements with SIMS. We had three objectives: 1) To test whether SIMS-determined  $\text{OH}/^{16}\text{O}$  ratios can be used as a proxy for the organic content in otoliths at the ~200 picogram sampling scale provided by SIMS; 2) to assess whether intra-otolith organic content biased  $\delta^{18}\text{O}$  values measured by SIMS analyses of otoliths from a population of wild fish; and 3) to suggest a possible correction strategy for the organic-derived oxygen component within individual SIMS  $\delta^{18}\text{O}$  results. We

hypothesize that i) the spatial distributions of element ratios indicative of organic materials (P, S and  $\text{OH}/^{16}\text{O}$  ratios) vary similarly and in a predictable way within otoliths, showing banding patterns corresponding to annual growth zones; ii) concentrations of P, S and the  $\text{OH}/^{16}\text{O}$  ratio decrease with increasing age and size of the otolith, covarying with increasing  $\delta^{18}\text{O}$  values from core to margin; and iii) intraotolith  $\delta^{18}\text{O}$  values show an inverse relationship with  $\text{OH}/^{16}\text{O}$  values, leading to lower  $\delta^{18}\text{O}$  values in growth zones containing large amounts of organic matter.

## 2. Materials and methods

### 2.1. Study site & sampling

We sampled 113 pike (*Esox lucius*) from three major brackish lagoon chains (n = 54) and freshwater tributaries (n = 53) around Rügen island in the southern Baltic Sea, Germany. (Fig. 1). To represent different habitats and abiotic conditions, pike were sampled along environmental gradients of salinity and temperature (Figure S1). We aimed for equal size and sex distributions, however, equal sex distribution was not achieved due to sex-dimorphic growth in pike (Casselman, 1995, but see also Figure S2, S3). Additionally, we sampled five individuals from Lake Kleiner Döllensee (4 females, 1 male, Fig. 1), a dimictic lake with 25 ha surface area and a mean depth of 4.1 m, situated around 150 km from the main study area, which we used as a reference site with no connection to the lagoons. To account for gear-dependent size- and growth-selectivity, pike were sampled with different gears, including fyke nets, gill nets, rod and line fishing and electrofishing in tributaries (Table S1). Each fish was euthanized, measured for total length, sex determined, and the head was frozen for processing in the lab. We extracted sagittal otoliths from all 113 pike, and measured each individual otolith for lifelong  $\delta^{18}\text{O}$  and  $\text{OH}/^{16}\text{O}$  values with SIMS (Table 1). SIMS data of all 113 fish were then used for linear mixed effects modelling and the development of a pairwise correction (Table 1). A subsample of three individuals were chosen for EPMA scans of potential trace elemental proxies of organic content (Table 1). BH-01855, a seven-year-old male pike sampled from WRBC (Fig. 1) in May 2020 at 72.2 cm total length; BH-01588, a 10-year-old female pike sampled from NRBC (Fig. 1) in January 2020 with 105.0 cm total length; and BH-01722, a 13-year-old female pike sampled from NRBC in February 2020 at 95.0 cm total length. Out of these three specimen, BH-01588 was chosen for a SIMS grid measurement and subsequent interpolation of  $\delta^{18}\text{O}$  across the otolith surface (Table 1). Pike used in this study exhibited three behavioral phenotypes: 55 individuals permanently inhabited brackish lagoons, 32 individuals permanently inhabited freshwater tributaries (or the inland lake), and 26 regularly migrated between brackish and freshwater (for detailed characterization of the behavioral phenotypes, see Rittweg et al., 2024)

### 2.2. Otolith processing and SIMS analyses

Sagittal otoliths were extracted and cleaned, dried in a desiccator for 48 h, then stored under atmosphere in the laboratory. Otoliths were glued onto glass slides with Crystalbond glue and cut into 100 µm thin sections using an Isomet low-speed saw (BUEHLER Ltd 11–1180). The Crystalbond was then dissolved in acetone, resulting free otolith sections were polished with 3000 and 5000 grit sandpaper and 0.3 µm lapping film, and sent to the SIMS facility at the German Research Center for Geosciences (GFZ), Potsdam. Thin sections were embedded in 1-inch diameter, round epoxy sample mounts using Epofix resin (STRUERS), along with the UW3 and IAEA603 calcite reference materials (Kozdon et al., 2009, International Atomic Energy Agency, 2016). Resulting mounts were polished until a surface quality of <5 µm was reached, which was verified with white-light profilometry. Mounts were imaged with an optical microscope using both reflected light and dark field modes, then sputter-coated with a 35-nm high-purity gold film to assure

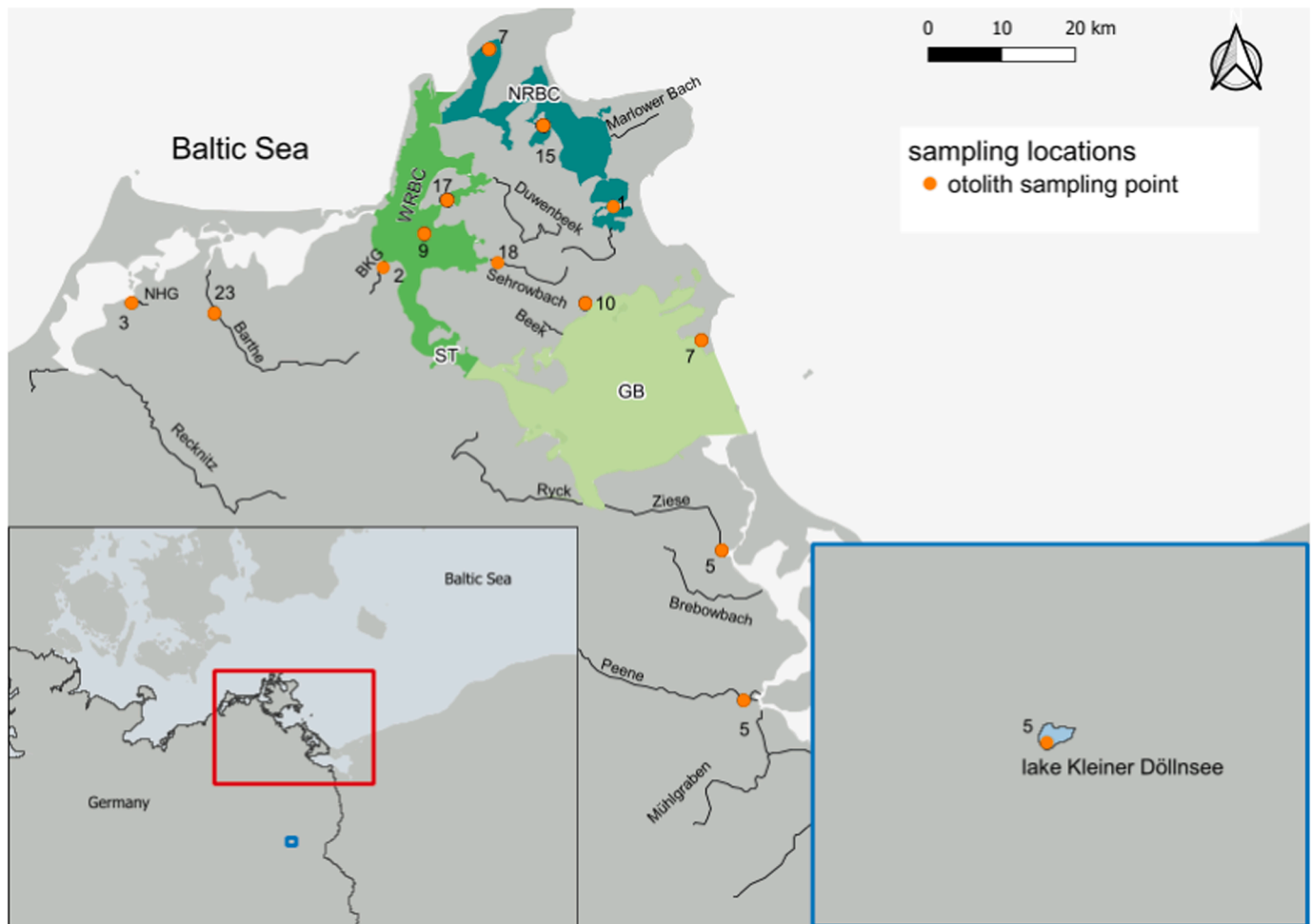


**Fig. 1.** Sampling Locations for pike captured between July 2019 and April 2022 in brackish lagoons and freshwater tributaries around Rügen island in northern Germany (large map), and in the freshwater lake Kleiner Döllnsee in Brandenburg (right inset map). Numbers beside the sampling points refer to the number of fish captured at a given location. NRBC: North Rügen Bodden chain; WRBC: West Rügen Bodden chain; GB: Greifswalder Bodden; ST: Strelasund; NHG: Neuendorfer Hechtgraben; BKG: Badendycksgraben.

**Table 1**

Overview of sample sizes, sex ratio (f = female, m = male), size and age range of pike individuals per analysis method. All fish were captured between July 2019 and May 2022 from brackish lagoons and freshwater tributaries around Rügen island in northern Germany, and the reference freshwater lake Kleiner Döllnsee in northern Germany.

Method	Total N (f, m)	Size (cm)	Mean size $\pm$ SD (cm)	Period	Age (years)
SIMS	113 (70, 43)	40.4 – 126.2	72.9 $\pm$ 17.1	2019–2022	1–13
Mixed linear models	113 (70, 43)	40.4 – 126.2	72.9 $\pm$ 17.1	2019–2022	1–13
$\delta^{18}\text{O}$ correction	113 (70, 43)	40.4 – 126.2	72.9 $\pm$ 17.1	2019–2022	1–13
EPMA	BH–01855 (m)	72.2	NA	2020	7
	BH–01588 (f)	105.0	NA	2020	10
	BH–01722 (f)	95.0	NA	2020	13
SIMS grid	BH–01588 (f)	105.0	NA	2020	10

electrical conductivity. The mounts were then placed in a specially designed high-vacuum storage chamber of the Cameca 1280-HR secondary-ion mass spectrometer (details in Rittweg et al., 2023).  $\delta^{18}\text{O}$  and  $\text{OH}/^{16}\text{O}$  values were determined along transects which were marked digitally on otolith sections covering a straight line from otolith core to distal edge along an axis crossing all visible annuli. Transects were determined as point measurements with step distances of  $\sim 35 \mu\text{m}$ , with UWC3 and IAEA603 calcite reference materials determined after each 10th measurement. Results were corrected for instrumental mass fractionation and instrumental drift and the  $\delta^{18}\text{O}$  values were reported in ‰ relative to Vienna Standard Mean Ocean Water (VSMOW), and converted to ‰ relative to Vienna Pee Dee Belemnite (VPDB) reference

scale using the equation of Brandt et al. (2014). In order to determine the relative abundances of hydrogen, which is a proxy for the amount of protein-bound oxygen included in a given analysis, we determined the  $\text{OH}/^{16}\text{O}$ -ratios as part of each 80 second integration. Briefly, the  $\text{OH}$ -intensity was determined using the mono-collection Faraday Cup detector with an e12 Ohm amplifier while the  $^{16}\text{O}$ -count rate was determined concurrently using the L2' Faraday cup with an e10 Ohm amplifier. The reported  $\text{OH}/^{16}\text{O}$ -values were derived by dividing one count rate by the other without any attempt to calibrate for absolute hydrogen contents - hence the values only provide relative abundances between analytical locations. To assess the spatial distribution of  $\delta^{18}\text{O}$  and  $\text{OH}/^{16}\text{O}$  values and to validate  $\text{OH}/^{16}\text{O}$  as proxy for organic

**Table 2**

Effects of fixed and random predictors on linear mixed models of z-transformed  $\delta^{18}\text{O}$  values measured in transects extending between otolith core and otolith margin in 113 pike otoliths sampled from specimens captured between July 2019 and May 2022 from brackish lagoons and freshwater tributaries around Rügen island in northern Germany, and the reference freshwater lake Kleiner Döllnsee in northern Germany.

scaled $\delta^{18}\text{O}$ (marginal $R^2 = 0.52$ ; conditional $R^2 = 0.68$ ) <sup>a</sup>				
Predictors	Estimate ( $\pm$ SE)	t-value	LLR	p-value
Intercept	-0.47 (0.13)	-3.56		
<b>OH count rate</b>	<b>-0.36 (0.02)</b>	<b>-18.58</b>	<b>316.65</b>	<b>&lt; 0.001 ***</b>
<b>distance from core</b>	<b>0.74 (0.20)</b>	<b>25.34</b>	<b>604.03</b>	<b>&lt; 0.001 ***</b>
<b>increment width</b>	<b>0.18 (0.07)</b>	<b>2.50</b>	<b>5.71</b>	<b>&lt; 0.05 *</b>
capture location [freshwater]	-0.13 (0.17)	-0.80		
<b>phenotype [freshwater resident]</b>	<b>-2.92 (0.21)</b>	<b>-14.00</b>	<b>121.34</b>	<b>&lt; 0.001 ***</b>
<b>phenotype [brackish resident]</b>	<b>-1.83 (0.27)</b>	<b>-6.91</b>	<b>121.34</b>	<b>&lt; 0.001 ***</b>
sex [male]	0.11 (0.09)	1.31		
<b>Random Effects</b>	<b>Variance (<math>\pm</math> SD)</b>		<b>LLR</b>	<b>p-value</b>
<b>ID</b>	<b>0.18 (0.42)</b>		<b>994.53</b>	<b>&lt; 0.001 ***</b>
Residual	0.37 (0.61)			

SE: Standard error; SD: Standard deviation; LLR: Log-likelihood ratio. Significant effects are shown in bold.

<sup>a</sup> Marginal  $R^2$  describes the proportion of the total variance explained by fixed effects in the model; conditional  $R^2$  describes the proportion of total variance explained by fixed and random effects combined in the model.

contributions, 818 SIMS measurements were performed in an evenly spaced grid pattern with a  $35 \times 35 \mu\text{m}$  step size covering the distal portion of the otolith thin section of specimen BH-01588, a 10-year-old female pike sampled from NRBC in January 2020 with 105.0 cm total length. To assess the spatial distribution of  $\delta^{18}\text{O}$  and  $\text{OH}/^{16}\text{O}$ , inverse probability weighted (IPW) interpolations were produced from the grid pattern of the otolith specimen BH-01588.

### 2.3. EPMA analysis

Following SIMS analysis, the gold coating was removed from each mount using ethanol and polishing powder (Alpha alumina, 300 nm). The mounts were sent to the electron microprobe facility at GEOMAR Helmholtz Center for Ocean Research, Kiel. The three chosen specimen samples were sputter-coated with high-purity carbon and analyzed using a JEOL JXA 8200 electron microprobe. The microprobe was calibrated with KAN1, VG-2, apatite, sphalerite, strontianite, dolomite, and calcite reference materials. A  $10 \times 10 \mu\text{m}$  grid covering each of the three selected otoliths was determined for the elements calcium (Ca), phosphorus (P), sulfur (S), magnesium (Mg), and strontium (Sr). The  $\delta^{18}\text{O}$  and  $\text{OH}/^{16}\text{O}$  interpolations determined with SIMS for specimen BH-01588 were visually compared to bitmap images from EPMA scans of the same otolith showing the concentrations of the organic proxies P and S.

### 2.4. modelling intraotolith $\delta^{18}\text{O}$ and $\text{OH}/^{16}\text{O}$ values

To assess the impact of organic contributions along  $\delta^{18}\text{O}$  line transects across the whole sample ( $n = 113$  otoliths), we fitted linear mixed effects models predicting lifelong individual  $\delta^{18}\text{O}$  values from a set of fixed and random predictors.  $\text{OH}/^{16}\text{O}$  ratios, our proxy for organic content, was included as a fixed predictor. To account for effects of different growth, we included increment width (width of annual rings) as a fixed predictor. To account for effects associated with the body size of individual fish, we included distance from the otolith core as a proxy of body size as fixed predictor. To account for effects associated with differences in salinity between capture locations, capture location was included as fixed predictor. To control for the effect of ontogenetic

habitat shifts, behavioral phenotype (resident freshwater, resident brackish or migratory) was included as fixed predictor. To test for possible effects of sex, sex was also included as a fixed effect. Individual fish ID was included as a random predictor, to account for the repeated measures design. To correct for differences in scale,  $\delta^{18}\text{O}$  and  $\text{OH}/^{16}\text{O}$  values were z-scored and mean-centered prior to modeling. Log likelihood ratio (LLR) tests were used to assess the significance of fixed and random effects; we have reported marginal and conditional  $R^2$  estimates as measures of goodness-of-fit. Assumptions of the model were assessed graphically (supplementary material section C).

### 2.5. Correcting for the effect of organics on $\delta^{18}\text{O}$

Using the coefficients from a linear best-fit regression of  $\text{OH}/^{16}\text{O}$ -ratios vs  $\delta^{18}\text{O}$ , we developed an individual-level correction of  $\delta^{18}\text{O}$  values. Extracting the calculated regression slope estimate for the effect of  $\text{OH}/^{16}\text{O}$ -ratios on measured  $\delta^{18}\text{O}$  values across all fish, we calculated a corrected  $\delta^{18}\text{O}$  value for each measurement point using the formula:

$$\delta^{18}\text{O}_{\text{corrected}} = \delta^{18}\text{O}_{\text{otolith}} - \text{OH}/^{16}\text{O} \times \text{population slope coefficient}$$

The results of these corrections were assessed as average offset across the whole sample ( $n = 113$ ) at the population level, distinguishing capture location and life history strategy. Furthermore, we examined the individual level offsets across the three specimens that were selected for EPMA analysis by plotting them individually with corrected and uncorrected values.

To validate our correction, we used water  $\delta^{18}\text{O}$  measurements and time series of water temperatures for the lagoons to predict theoretical monthly  $\delta^{18}\text{O}$  values in pike otoliths between 2008 and 2022 (age range of our sample). Monthly variation in water  $\delta^{18}\text{O}$  was determined from biweekly samples between March 2020 and March 2021 taken by Aichner et al. (2022), and interpolated for each lagoon region across the time span from 2008 to 2022. We used two fractionation equations to predict  $\delta^{18}\text{O}$  in pike otoliths, as no species-specific equation exists for pike, and the coastal lagoons cannot be easily classified as fully marine or fully freshwater. Eq. 1 was developed as general fractionation equation for freshwater fish (Patterson et al., 1993), Eq. 2 was developed for a marine species (plaice, *Pleuronectes platessa*, Geffen, 2012). The two



equations took the form:

$$1000\ln\alpha = 18.56(1000T(K)^{-1}) - 33.49 \quad (1)$$

$$\text{where } \alpha = \frac{1000 + \delta^{18}\text{O}_{\text{oto}} \text{VSMOW}}{1000 + \delta^{18}\text{O}_{\text{water}} \text{VSMOW}}$$

and

$$1000\ln\alpha = 15.99(1000T(K)^{-1}) - 24.25 \quad (2)$$

$$\text{where } \alpha = \frac{1000 + \delta^{18}\text{O}_{\text{oto}} \text{VSMOW}}{1000 + \delta^{18}\text{O}_{\text{water}} \text{VSMOW}}$$

where T is temperature in Kelvin (K),  $\alpha$  is the fractionation factor between water  $\delta^{18}\text{O}$  and otolith  $\delta^{18}\text{O}$ . A linear interpolation of  $\delta^{18}\text{O}$  values measured in pike otoliths was used to interpolate to a period of 12 months within identified annuli to facilitate comparison to predicted values. Predicted, raw and corrected  $\delta^{18}\text{O}$  values were compared graphically. Some error was expected from matching sample locations within otoliths to months and interpolation errors. Incorporating the variance in water temperatures across lagoons and water  $\delta^{18}\text{O}$  values across seasons into the interpolations allowed us to construct upper and lower confidence intervals for predicted otolith  $\delta^{18}\text{O}$  for the two equations.

### 3. Results

#### 3.1. Distribution patterns of elemental proxies

The spatial distribution of phosphorus (P) and sulfur (S) correlated closely with annual bands of slow and fast growth in the three otolith specimen (Figures S4 - S6). P and S were concentrated within summer growth zones, with maximum concentrations of 12.1 % (percent weight) for P and 3.6 % for S (Figures S4 - S6). Concentrations of P and S decreased from the otolith core outwards in all three otoliths (Figures S4 - S6). Concentrations of Mg were low, ranging from 0 % to 1.9 %, leading to no clear banding in the EPMA images (Figures S4 - S6).

The two-dimensional spatial interpolations of  $\delta^{18}\text{O}$  and  $\text{OH}/^{16}\text{O}$  values of otolith BH-01588 showed a clear banding pattern in  $\delta^{18}\text{O}$  values, corresponding to summer and winter growth zones (Fig. 2). The banding in  $\text{OH}/^{16}\text{O}$  ion count ratios was less pronounced, however, higher  $\text{OH}/^{16}\text{O}$  count ratios near the otolith core corresponded to areas with generally lower  $\delta^{18}\text{O}$  (Fig. 2), indicating that the correlation between  $\delta^{18}\text{O}$  values and  $\text{OH}/^{16}\text{O}$  extended across the otolith from core to margin.

#### 3.2. Correlation between organic proxies

The organic proxies P and S appeared to broadly correlate with SIMS point profiles of both  $\delta^{18}\text{O}$  and  $\text{OH}/^{16}\text{O}$  ratios (Figure S7 - S9). Higher concentrations of P and S in summer growth zones often coincided with higher  $\text{OH}/^{16}\text{O}$  ratio in SIMS point profiles, but more importantly, the overall decrease in P and S from core region towards the otolith margin coincided with an increase in  $\delta^{18}\text{O}$  values and a decrease in  $\text{OH}/^{16}\text{O}$  ratio across all three sample otoliths (Figure S7 - S9). This relationship was also found for the spatial distribution of P, S,  $\delta^{18}\text{O}$  and  $\text{OH}/^{16}\text{O}$  (Fig. 2). This suggests that the  $\text{OH}/^{16}\text{O}$  ratio is a useful proxy for organic content in fish otoliths. We assumed this to hold true for our larger sample ( $n = 113$  pike otoliths) and used  $\text{OH}/^{16}\text{O}$  ratio as a predictor for  $\delta^{18}\text{O}$  values in subsequent modelling steps (see below).

#### 3.3. Modelling intraotolith $\delta^{18}\text{O}$ values

The best-performing model for correcting our  $\delta^{18}\text{O}$  values included  $\text{OH}/^{16}\text{O}$  ratio (continuous, z-transformed), distance from otolith core (continuous) as a measure of age, increment width (continuous) as a measure of yearly growth, behavioral phenotype (factor with three levels, freshwater resident, brackish resident, migratory) capture location (factor with two levels, lagoon/tributary) and sex (factor, two levels male/female) and the random effect of individual ID (1 ID, 112 groups). The model explained 68 % of the variance in intra-otolith  $\delta^{18}\text{O}$  values, where 52 % of the variance was explained by the fixed predictors (Table 2). This indicated a large amount of variation in  $\delta^{18}\text{O}$  values was due to inter-individual variation, reflecting differences in life history between individual pike. Accordingly, the random effect of ID was highly significant (Table 2). Scaled  $\text{OH}/^{16}\text{O}$  ratios had a significant negative effect on scaled  $\delta^{18}\text{O}$  values (Table 2, Fig. 3). Age and body size had a positive effect on  $\delta^{18}\text{O}$  values, as indicated by a highly significant positive correlation between scaled  $\delta^{18}\text{O}$  and distance from the otolith core (Table 2, Fig. 4). Fish growth rate, as inferred by otolith increment widths, also showed a positive effect on  $\delta^{18}\text{O}$  values (Table 2). As expected, behavioral phenotype was a significant predictor of intraotolith  $\delta^{18}\text{O}$ , with freshwater-resident and migratory pike showing lower  $\delta^{18}\text{O}$  values than brackish residents (Table 2). Male and female pike did not differ in intra-otolith  $\delta^{18}\text{O}$  values, indicated by a non-significant fixed effect of sex on scaled  $\delta^{18}\text{O}$  values (Table 2).

#### 3.4. Correcting for organic effects on SIMS determinations of $\delta^{18}\text{O}$

Applying a mathematical correction based on paired  $\delta^{18}\text{O}$  values and  $\text{OH}/^{16}\text{O}$  ratios resulted in a mean offset of 0.54 ‰ in  $\delta^{18}\text{O}$  values across all 113 pike. Average offsets between the uncorrected  $\delta^{18}\text{O}$  values and the corrected values differed significantly between behavioral phenotypes (One-way ANOVA,  $F_{2,4604} = 596.6$ ,  $p < 0.001$ ), with lagoon-captured pike showing the highest average offset (+ 0.59 ‰, Fig. 4), followed by migratory anadromous individuals (+ 0.52 ‰, Fig. 3), and freshwater-resident pike showing the lowest average offset (+ 0.48 ‰, Fig. 4), suggesting some variance was induced by different habitat use of individual fish. The strongest offsets across all fish were detected in near-core areas of otoliths, with an average offset of + 1.1 ‰ in the first 500  $\mu\text{m}$  of the otolith, which corresponds to larval or juvenile life stages.

The magnitude of the correction differed strongly between individuals, as some individuals exhibited intra-otolith  $\delta^{18}\text{O}$  determinations that were corrected by a maximum of 0.5 ‰, while other individuals showed shifts by up to 1 ‰ (Fig. 6). Of the three pike otoliths chosen for EPMA mapping, the otoliths BH-01588 and BH-01855 showed large differences between raw and corrected  $\delta^{18}\text{O}$  values, in particular in their near-core regions (Fig. 6). This was in accordance with the steep concentration gradient found in P and S for these two specimens (Figure S7, S8). The  $\delta^{18}\text{O}$  values of BH-01722 changed comparatively little after applying the correction (Fig. 6), which can be attributed to the rather low and homogenous P and S contents found in this otolith (Figure S9). Our correction shifted  $\delta^{18}\text{O}$  values in pike otoliths closer to the theoretical prediction intervals calculated from monthly water temperatures and interpolated water  $\delta^{18}\text{O}$  values between 2008 and 2022 (Fig. 5). Corrected  $\delta^{18}\text{O}$  values lay within the confidence intervals of the two predictions from Eqs. 1 and 2 for most of the year, although some offset between corrected and predicted  $\delta^{18}\text{O}$  values remained in the coldest months of the year, where the highest  $\delta^{18}\text{O}$  values were predicted (Fig. 5).

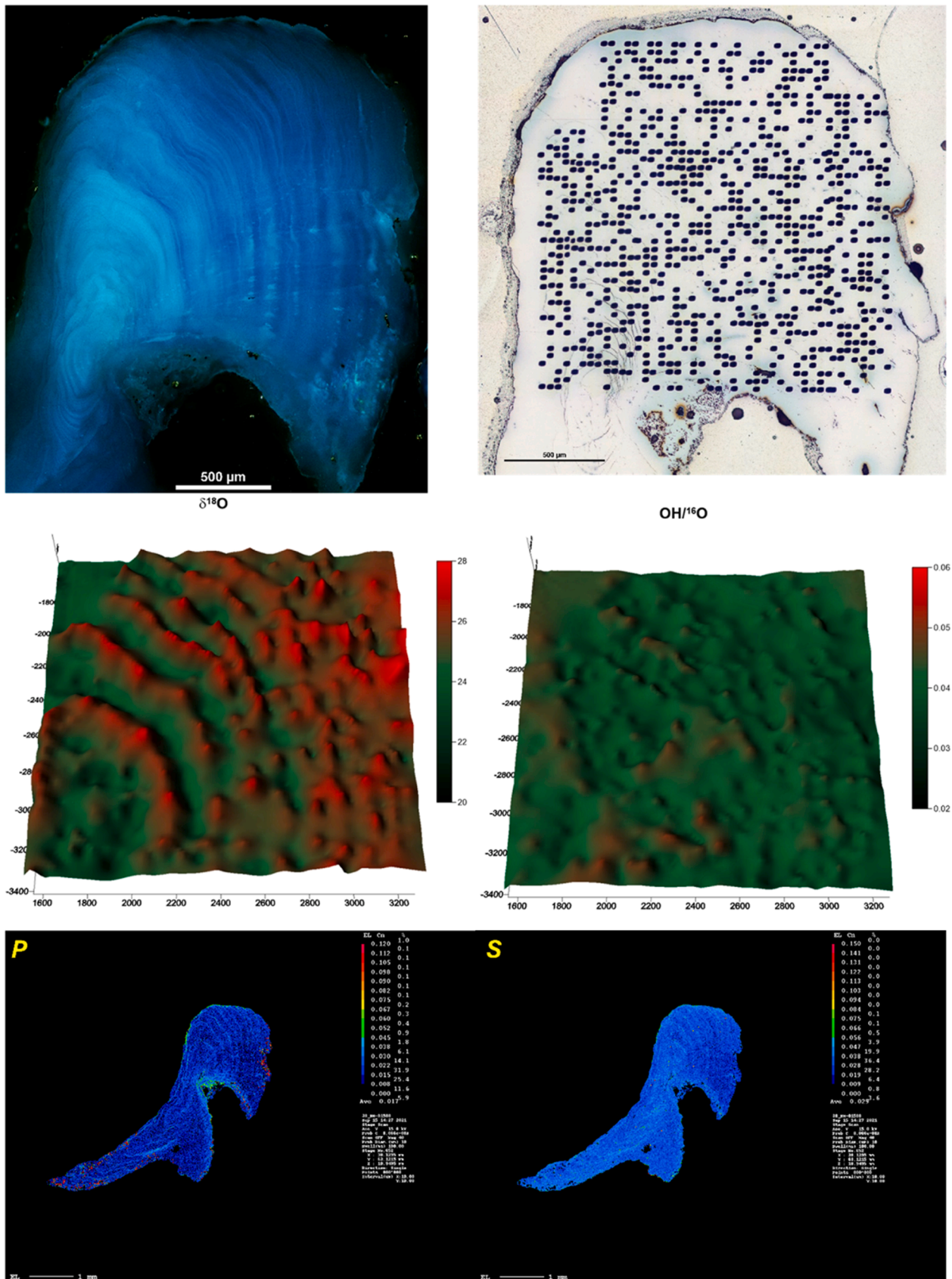
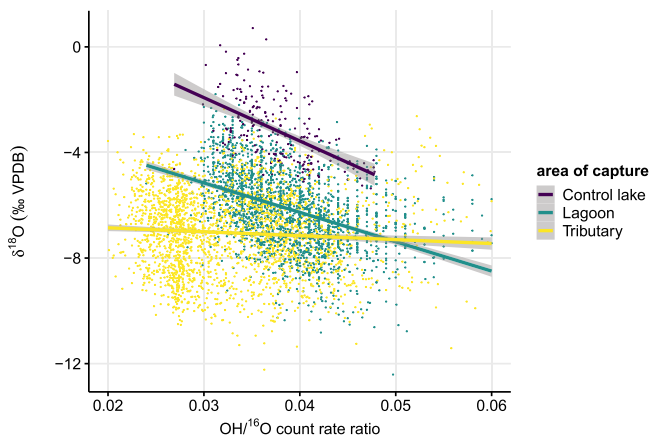
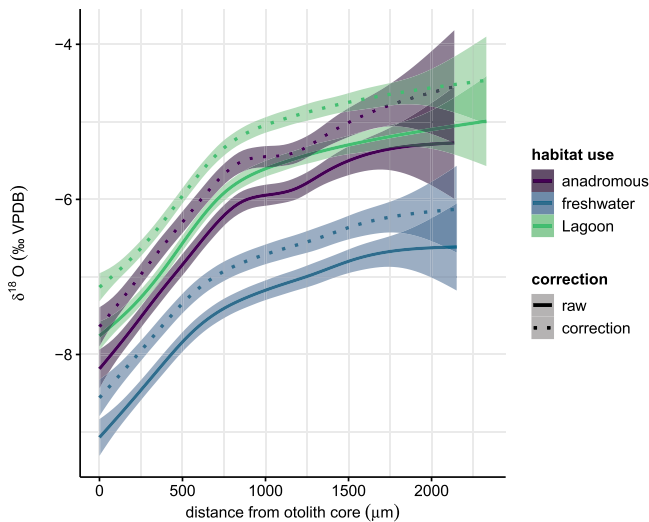


Fig. 2. SIMS interpolation of  $\delta^{18}\text{O}$  values (middle left panel) and  $\text{OH}/^{16}\text{O}$  ion counts (middle right panel) of pike otolith specimen BH-01588, a 10-year-old female pike sampled from NRBC in February 2020 at 105 cm total length. For orientation, we included the optical dark field image of the otolith prior to measuring the SIMS grid pattern (upper left panel), and the bright field image of the otolith taken after the SIMS grid pattern was measured (upper right panel). Lower panels show the EPMA maps of the entirety of the same otolith.



**Fig. 3.** Correlation between SIMS determined  $\delta^{18}\text{O}$  values and  $\text{OH}/^{16}\text{O}$  ratios in 113 pike captured between July 2019 and May 2022 from brackish lagoons and freshwater tributaries around Rügen island in northern Germany and a reference freshwater lake 150 km inland.



**Fig. 4.** Corrected vs. uncorrected intraotolith  $\delta^{18}\text{O}$  values from 113 otoliths from pike sampled between July 2019 and May 2022 in brackish lagoons and several freshwater tributaries around Rügen island in northern Germany and a reference freshwater lake 150 km inland. Individuals were grouped based on their lifelong habitat use behavior, with lagoon-residing pike in green, migratory (anadromous) individuals in purple and freshwater resident pike in blue. Solid lines show the raw  $\delta^{18}\text{O}$  measurements, dashed lines show the values after applying the correction. Shaded areas represent the 95 % confidence intervals around the smoothing lines.

#### 4. Discussion

We determined the relationship between intraotolith  $\delta^{18}\text{O}$  values and several organic tracers for pike otoliths and derived a mathematical correction for SIMS  $\delta^{18}\text{O}$  values using paired measurements of  $\text{OH}/^{16}\text{O}$  and  $^{18}\text{O}/^{16}\text{O}$ . We demonstrated the effect of organic components was constant across a variety of habitat use strategies in an ecologically plastic species (Dhellemmes et al., 2023; Rittweg et al., 2024; Sunde et al., 2022). According to our first hypothesis, the organic content in otoliths was associated with seasonal growth zones, with opaque summer growth zones showing higher concentrations of proxies associated with organic phases, such as P and S. While this was the case for the two organic proxies P and S, in support of our hypothesis, we were not able to detect a clear annual banding in  $\text{OH}/^{16}\text{O}$  counts, potentially due to other physiological mechanisms affecting organic content. In general,

however, the concentrations of organic proxies decreased from otolith core towards margin across all three samples analyzed by EPMA, which supported our second hypothesis. In response to our third hypothesis, we detected a significant inverse linear relationship between  $\text{OH}/^{16}\text{O}$  and  $\delta^{18}\text{O}$  values, which was influenced by growth rate, capture location and fish age. Applying a pairwise individual-level correction of  $\delta^{18}\text{O}$  using  $\text{OH}/^{16}\text{O}$ , we determined an average 0.54 ‰ shift in  $\delta^{18}\text{O}$  values due to the admixture of organic-bound oxygen to otolith carbonate. The correction shifted otolith  $\delta^{18}\text{O}$  values of pike closer towards theoretically expected values predicted from ambient temperatures and water  $\delta^{18}\text{O}$ , suggesting the offset between measured and expected value was due to intraotolith organics.

The decrease in elements associated with organics, specifically S and P, as well as the trend towards lower  $\text{OH}/^{16}\text{O}$  from core to margin reflect decreasing growth rates and consequentially lower organic content (Hüssler et al., 2004) with increasing age in fishes (von Bertalanffy, 1938). The similar spatial distributions in P, S and  $\text{OH}/^{16}\text{O}$  indicated that  $\text{OH}/^{16}\text{O}$  ratios also record organic content in otoliths, and can be used as a quantitative indicator for the organic content in aragonite. The higher organic contents found in the core regions followed our expectations, as pike are known to grow fast in early life, with growth rates slowing with onset of maturity (Bry et al., 1991; Pagel et al., 2015). Behavioral phenotype was a strong predictor of intra-otolith  $\delta^{18}\text{O}$  values, which can be explained by freshwater tributaries being depleted in  $^{18}\text{O}$  compared to brackish lagoons, which consist of a mixture of isotopically heavy ocean water and isotopically light freshwater (Aichner et al., 2022). Therefore, individuals that spend parts of their life cycle (migratory anadromous), or their whole life cycle (brackish residents) in brackish lagoons were expected to show overall higher  $\delta^{18}\text{O}$  values. Direction and magnitude of the relationship between  $\delta^{18}\text{O}$  and  $\text{OH}/^{16}\text{O}$  was consistent between habitats and behavioral phenotypes, indicating the negative correlation did not result from habitat-related effects. However, pike from our reference lake showed much higher  $\delta^{18}\text{O}$  values than any other fish in the sample, despite it being a pure freshwater lake. A possible explanation for this could be strong evaporation effects on the lake, which has only neglectable in- and outflow, and therefore receives little groundwater input to balance out  $\delta^{18}\text{O}$  enrichment through evaporation (Horton et al., 2015). This may drive  $\delta^{18}\text{O}$  values towards more positive values (Aichner et al., 2022), which would also be reflected in fish otoliths.

The inverse relationship between organic matter (approximated by  $\text{OH}/^{16}\text{O}$ ) and  $\delta^{18}\text{O}$  values seen in our study agrees with previous work on fish otoliths (Guiguer et al., 2003; Hane et al., 2020, 2022; Matta et al., 2013), and also with more general studies on isotope measurements (Oehlerich et al., 2013). This effect likely results from the scale conversion between reference scales - Standard Mean Ocean Water (SMOW) and Pee Dee Belemnite (PDB) - which have commonly been used to report the small isotopic variations in organic (SMOW) or inorganic (PDB) materials. The conversion between the scales is  $\delta^{18}\text{O}_{\text{VPDB}} = 0.97001 \times \delta^{18}\text{O}_{\text{VSMOW}} - 29.99$  (Brandt et al., 2014).

Water (and organic-bound oxygen derived from body water) is typically expressed relative to SMOW, and thus, when expressed on the VPDB scale, becomes 29.99 ‰ lighter. Consequently, when organic-bound oxygen with  $\delta^{18}\text{O}_{\text{VSMOW}}$  values close to 0 ‰, but  $\delta^{18}\text{O}_{\text{VPDB}}$  values closer to -30 ‰ are determined together with mineral carbonate, the organic fraction drives the overall  $\delta^{18}\text{O}$  value lower. However, the extent to which otolith  $\delta^{18}\text{O}$  values are influenced by organic-bound oxygen appears to be variable, ranging from 3.7 ‰ in Guiguer et al. (2003) to 1 ‰ in Matta et al. (2013), to 0.41 ‰ in Hane et al. (2020). Our results suggested an average shift in  $\delta^{18}\text{O}$  values of 0.52 ‰, which is close to the offset reported by Hane et al. (2020), but we found the offset values to vary significantly between individuals and across behavioral phenotypes. This variability in offsets might be explained by our correction being based on paired values of an organic proxy that allowed the correction to change across individual otolith transects. The overall differences in mean offsets between studies suggested species-level



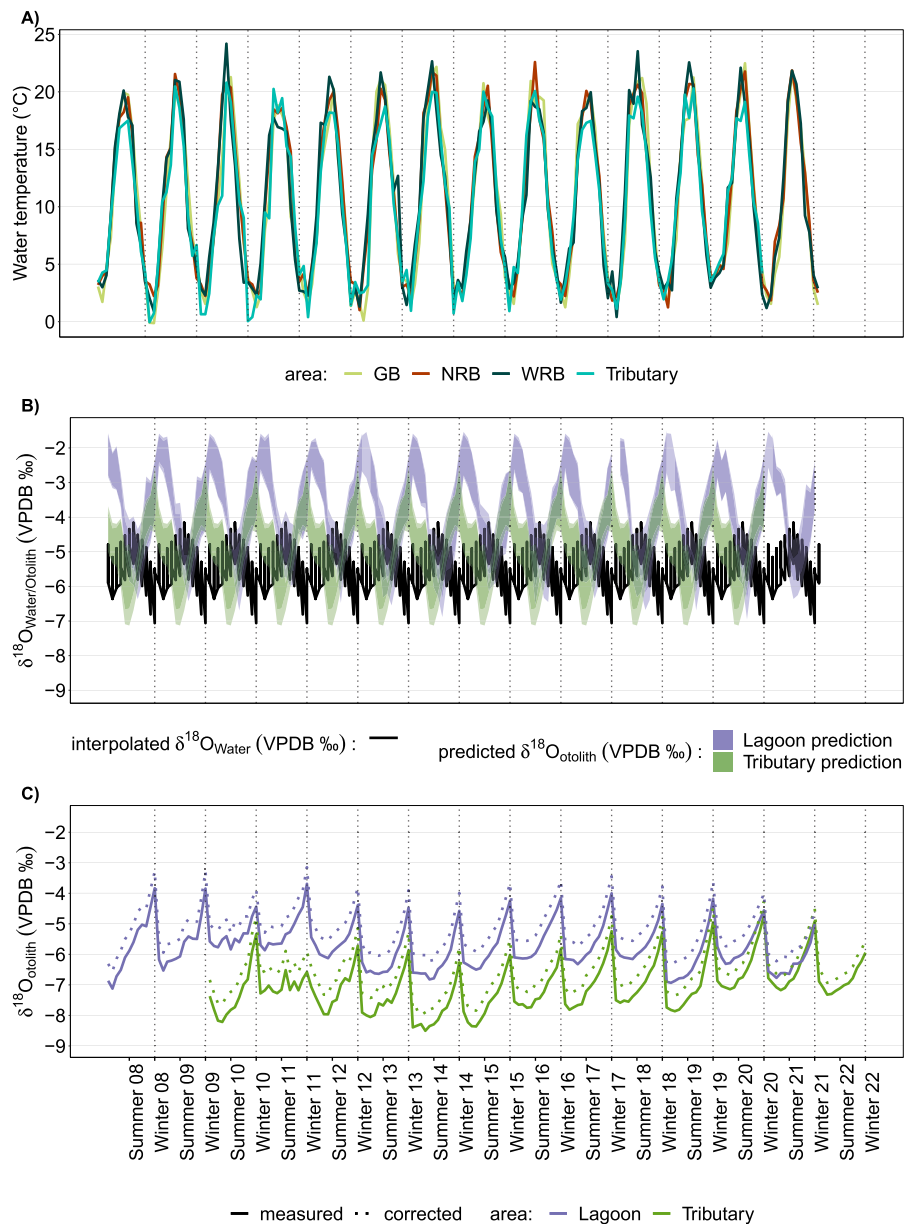


**Fig. 5.** A) Water temperature between January 2008 and December 2022 for the lagoon chains Greifswalder Bodden (GB), Northern Rügen Bodden Chain (NRB), Western Rügen Bodden Chain (WRB) and several tributaries, averaged across all tributaries (data source: LUNG MV). B) Water  $\delta^{18}\text{O}$  values interpolated from time series (March 2020 to March 2021) and transect measurements (June 2019, March 2020 and July 2020) by Aichner et al. (2022), along with theoretical otolith  $\delta^{18}\text{O}$  values calculated via fractionation equations from water  $\delta^{18}\text{O}$  and temperatures (Geffen, 2012; Patterson et al., 1993). C) Raw (solid lines) and corrected (dotted lines)  $\delta^{18}\text{O}$  values for 113 otoliths from pike sampled between July 2019 and May 2022 in brackish lagoons and several freshwater tributaries around Rügen island in northern Germany. Individuals were grouped based on capture location brackish lagoon and freshwater tributary. Pike from the reference freshwater lake were excluded as we had no water  $\delta^{18}\text{O}$  data for the reference lake.

differences in intraotolith organic contents, rendering generalized offset corrections across species potentially unreliable.

In addition to the offsets induced by organic matter, SIMS  $\delta^{18}\text{O}$  determination may further be influenced by matrix effects. A bias favoring  $^{16}\text{O}$  ions has been reported when sputtering an organic matrix as compared to inorganic calcium carbonate during studies employing a nano-SIMS instrument (Oehler et al., 2009). Such an effect could partially explain the difference between species as the mass fraction of organic component would differ systematically between, e.g., species of fast vs slow growth and high vs. low metabolic rate. However, Guiguer et al. (2003) employed micro-drilling followed by phosphoric acid digestion to measure intra-otolith  $\delta^{18}\text{O}$  values and reported significant effects of organic content (up to 3.7 ‰) on  $\delta^{18}\text{O}$  values. Acid digestion is

free of matrix effects, confirming the offset between organic-rich and organic-poor materials in SIMS  $\delta^{18}\text{O}$  data cannot solely be due to matrix effects.

A final point to consider is that atmospheric water may be hygroscopically adsorbed onto otoliths when exposed to air. The organic lattice of the otolith consists of glycoproteins, i.e., proteins with covalently bound carbohydrate chains (Morales-Nin, 1986; Stevenson and Campana, 1992). Outer hydroxyl groups offer a site for water molecules to bind via hydrogen bonding. Amino acids, and in particular carbohydrate chains, are likely strongly hygroscopic compared to inorganic carbonates. During atmospheric storage of otoliths, this could result in atmospheric water molecules attaching to the outer OH groups of either the amino acids of the proteins or the carbohydrates through hydrogen



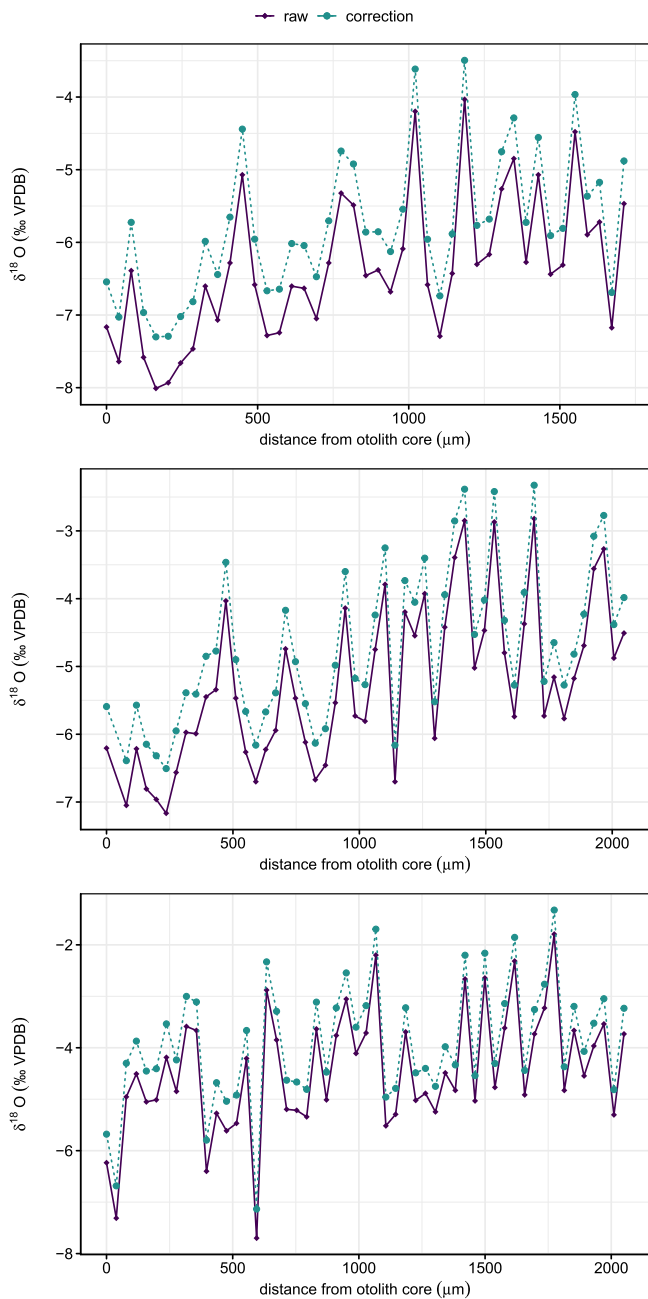


**Fig. 6.** Intraotolith  $\delta^{18}\text{O}$  values of the three example pike otoliths captured in May 2020 in brackish lagoons around Rügen island in northern Germany before (solid purple lines) and after (dashed green lines) applying the pairwise correction. Upper panel: BH-01855, a seven-year-old male pike sampled from WRBC in May 2020 at 72.2 cm total length; middle panel: BH-01588, a 10-year-old female pike sampled from NRBC in February 2020 at 105 cm total length; low panel: BH-01722, a 13-year-old female pike sampled from NRBC in February 2020 at 95.0 cm total length.

bonding. Additionally, water molecules from the atmosphere could also bind to imperfections in the aragonite crystal structure. Such imperfections are more common in areas of accelerated growth and higher organic content (Stevenson and Campana, 1992), potentially amplifying the effect. Oxygen in atmospheric water vapor is depleted in  $^{18}\text{O}$  relative to otolith carbonate, possibly altering  $\delta^{18}\text{O}$  measurements (Bowen et al., 2011). However, given that the upper 70–80 nm of otoliths used for our study were presputtered under vacuum, atmospheric water molecules would have had to diffuse into the otolith matrix down to around 100 nm, which we deemed unlikely. The possibility of otolith water

content influencing  $\delta^{18}\text{O}$  was also discussed by Hane et al. (2020), who compared SIMS-derived  $\delta^{18}\text{O}$  values to CF-IRMS, but this was not explicitly tested in Hane et al. (2020), nor in our study, suggesting avenues for further research.

Organic-induced offsets in  $\delta^{18}\text{O}$  may have significant implications for the reconstruction of ambient water temperatures from fish otoliths. Hane et al. (2020) indicated that the offset in  $\delta^{18}\text{O}$  values caused by organic matter content would result in an error in reconstructed temperatures of 1.5 °C in larval bluefin tuna. Other studies (e.g., Guiguer et al., 2003; Helser et al., 2018; Matta et al., 2013) suggest the potential bias in temperature reconstruction induced by varying organic contents might range between 1.5 °C and, in extreme cases, up to 13.5 °C. Using the commonly applied temperature fractionation equation of Patterson et al. (1993), the mean offset in  $\delta^{18}\text{O}$  values reported in our study (0.52 ‰), would result in an overestimation of temperature of  $\sim 1.9$  °C when applying  $\delta^{18}\text{O}$  thermometry. Furthermore, our results indicate stronger offsets for juvenile and larval stages, likely due to accelerated juvenile growth and higher organic matter content, potentially resulting in temperature overestimation of up to 4 °C for these early life stages. Early life stages are particularly vulnerable to environmental perturbations and represent a common bottleneck in recruitment and productivity of fish populations (Dahlke et al., 2020). Given the need to identify suitable spawning and nursery habitats for fisheries management (Reis-Santos et al., 2022), accurate environmental temperature reconstructions for early life stages are critical. Errors induced by offsets in  $\delta^{18}\text{O}$  could therefore lead to erroneous assessments of habitat suitability and resilience to warming.

Correcting SIMS  $\delta^{18}\text{O}$  values using paired OH/ $^{16}\text{O}$  values and the slope of a linear model of  $\delta^{18}\text{O}$  predicted by OH/ $^{16}\text{O}$  resulted in a decreasing offset with increasing distance from the otolith core. Applying this correction shifted pike otolith  $\delta^{18}\text{O}$  values closer towards theoretical values predicted by ambient temperatures and water  $\delta^{18}\text{O}$  values, validating the approach. However, differences remained between predicted and corrected values in the colder months of the year, where predicted  $\delta^{18}\text{O}$  was higher than corrected  $\delta^{18}\text{O}$ . This may be due to pike seeking thermal refuges, e.g., sheltered bays that are warmer than the open lagoons where the temperatures for the prediction were measured (Pursiainen et al., 2021), and active thermoregulation through sunbathing in pike (Nordahl et al., 2019), which would lead to lower otolith  $\delta^{18}\text{O}$  values than predicted by ambient water temperature. An alternative explanation could be errors introduced by the linear interpolation of otolith  $\delta^{18}\text{O}$  values over 12 months, as otoliths do not grow isometrically throughout the year (Stevenson and Campana, 1992). The magnitude of the correction varied between behavioral phenotypes, being lowest in freshwater resident pike and pike from the reference lake, likely due to slower juvenile growth of these individuals (Rittweg et al., 2024). Our results suggest that the relationship between organic content and  $\delta^{18}\text{O}$  values are more complex than anticipated previously, and may vary depending on growth dynamics and life history strategies. Unless the organic material can be quantitatively removed from the sample material prior to analysis, both SIMS and IRMS data may require correcting for the organic-derived oxygen (Guiguer et al., 2003; Hane et al., 2020). Roasting otoliths offers one possible solution, however, the effects of roasting on mineral composition (e.g., potential recrystallization of aragonite to calcite through heating) may be a problem for SIMS (Guiguer et al., 2003). We suggest that our correction approach based on paired  $\delta^{18}\text{O}$  values and OH/ $^{16}\text{O}$  ratios partially resolved the challenge associated with decreases in organic matter content with the increasing age of the fish. However, SIMS analysis is costly, and facilities with the necessary equipment for this method remain rare. Combining laser ablation inductively-coupled plasma mass spectrometry (LA-ICPMS) measurements of organic-bound trace elements, such as P, S, Cu, Zn, or Mn (Izzo et al., 2015), with commonly applied methods of measuring  $\delta^{18}\text{O}$ , such as micromilling (Helser et al., 2018), may present a cheap and more readily available method to assess influences of organic matter if SIMS is not an option. However, more research would be required before such correction methods become widely applicable.

#### 4.1. Limitations

The otoliths we used for our study were sampled from an area experiencing considerable isotopic variation in  $\delta^{18}\text{O}_{\text{Water}}$  over the course of a year due to mixing processes and seasonal differences in evaporation (Aichner et al., 2022). This might have introduced variation in intra-otolith  $\delta^{18}\text{O}$  which could contribute to the observed large differences between individual fish. Such environmental variation in oxygen isotopic ratio might further complicate our model, although this is unlikely to change the direction of the effects. Possible movements of individuals between habitats featuring different  $\delta^{18}\text{O}_{\text{Water}}$  values could further mask the impact of organics on  $\delta^{18}\text{O}_{\text{Otolith}}$ . However, we incorporated behavioral habitat use types described elsewhere (Rittweg et al., 2024) for fish in our model, which likely accounted for this possibility. Applying the correction led to different results for different capture locations and behavioral phenotypes, suggesting also other factors may have contributed to the observed effects, which our study did not fully resolve. Investigating the interaction of analytical and biological effects on SIMS  $\delta^{18}\text{O}$  determinations thus remains an important research topic that deserves further attention. The absence of clear seasonal bands in  $\text{OH}/^{16}\text{O}$  might indicate factors other than organic matter could contribute to this proxy, however, the negative association between  $\text{OH}/^{16}\text{O}$  and  $\delta^{18}\text{O}$  was strong across the entire sample, as was the positive association between  $\text{OH}/^{16}\text{O}$  and organic proxies across ontogeny, suggesting this proxy to be robust across the life history of an individual.

#### 4.2. Conclusions

Our study shows that, while the effect of organic contents on otolith  $\delta^{18}\text{O}$  was consistent with previous work, individual variability in habitat use, age and growth plays an important role, that has gone unrecognized. In our system, failing to account for the effect of organics on otolith  $\delta^{18}\text{O}$  values would result in overestimation of reconstructed temperatures by  $\sim 1.9^\circ\text{C}$ , which is ecologically significant. The ontogenetic effects revealed in our work lead us to advise caution when applying global corrections. If a correction is applied, non-constant, pairwise corrections, such as the equation proposed here, are biologically more realistic. Paired measurements of  $\text{OH}/^{16}\text{O}$  may be acquired without increasing the measuring time or cost during SIMS analyses, and a correction can be readily developed on a case-by-case basis. Where  $\delta^{18}\text{O}$  values are determined via acid dissolution, it is less clear how such a correction may be applied, although combined LA-ICPMS and micro-milling approaches may offer a potential solution, warranting further investigations. In either case it is clear that life history dynamics and habitat use of the target species need to be considered. Last, where it is practically possible, we recommend spatial assessments of different organic tracers on subsamples via EPMA scans or similar methods before analyzing otolith  $\delta^{18}\text{O}$ , to determine whether intraotolith organics may introduce bias.

#### Ethics approval

Fish were sampled in accordance with permit 7308.2 of the Landesamt für Landwirtschaft, Lebensmittelsicherheit und Fischerei (LALLF MV). Sampling in national park Vorpommersche Boddenlandschaft was carried out in accordance with permit 21/5320.142, Nationalparkamt Vorpommern, sampling in biosphere reserve Südost-Rügen was carried out in accordance with permit 5321.2/FM/SchnB.Nr.20002, Biosphärenreservatsamt. Sampling in nature reserves was carried out in accordance with permit 5328.1.99/654–19–40–3 of the Staatliches Amt für Landwirtschaft und Umwelt (STALU MV). Sampling of freshwater tributaries was carried out with permission by the Landesanglerverband Mecklenburg-Vorpommern e.V. (LAVB MV).

#### Funding

Deutsche Bundesstiftung Umwelt DBU, scholarship AZ20019/634; European Maritime and Fisheries Fund (EMFF), grant B 730117000069; State of Mecklenburg-Vorpommern, grant MV- I.18- LM- 004.

#### CRediT authorship contribution statement

**Timo Dustin Rittweg:** Writing – review & editing, Writing – original draft, Visualization, Project administration, Methodology, Investigation, Funding acquisition, Formal analysis, Conceptualization. **Michael Wiedenbeck:** Writing – review & editing, Validation, Software, Resources, Methodology, Data curation, Conceptualization. **Jan Fietzke:** Writing – review & editing, Validation, Software, Resources, Methodology, Data curation, Conceptualization. **Clive Trueman:** Writing – review & editing, Writing – original draft, Supervision, Investigation, Conceptualization

#### Declaration of Competing Interest

The authors declare no conflicts of interests.

#### Acknowledgements

We thank all commercial fishers and angling guides cooperating with project Boddenhecht for their kind assistance in sample collection. Uwe Dittmann is thanked for his expertise in preparing the SIMS sample mounts to the highest possible quality standard and Frédéric Couffignal is thanked for his careful attention to detail during SIMS data acquisition. We thank Karin Limburg and one anonymous reviewer for their valuable comments on the manuscript.

#### Appendix A. Supporting information

Supplementary data associated with this article can be found in the online version at doi:10.1016/j.fishres.2024.107239.

#### Data availability

Data used for the analysis are available from doi 10.18728/igb-fred-946.0, R code used for the analysis is available from <https://github.com/Traveller-2909/Otoganics>.

#### References

- Aichner, B., Rittweg, T., Schumann, R., Dahlke, S., Duggen, S., Dubbert, D., 2022. Spatial and temporal dynamics of water isotopes in the riverine-marine mixing zone along the German Baltic Sea coast. *Hydrol. Process.* 36 (9). <https://doi.org/10.1002/hyp.14686>.
- Bry, C., Hollebecq, M.G., Ginot, V., Israel, G., Manelphe, J., 1991. Growth patterns of pike (*Esox lucius* L.) larvae and juveniles in small ponds under various natural temperature regimes. *Aquaculture* 97 (2-3), 155–168. [https://doi.org/10.1016/0044-8486\(91\)90262-6](https://doi.org/10.1016/0044-8486(91)90262-6).
- Bowen, G.J., Kennedy, C.D., Liu, Z., Stalker, J., 2011. Water balance model for mean annual hydrogen and oxygen isotope distributions in surface waters of the contiguous United States. *J. Geophys. Res.* 116 (G4). <https://doi.org/10.1029/2010jg001581>.
- Burbank, J., Drake, D., Power, M., 2020. Field-based oxygen isotope fractionation for the conservation of imperilled fishes: an application with the threatened silver shiner *Notropis photogenis*. *Endanger. Species Res.* 42 (00), 83–93. <https://doi.org/10.3354/esr01040>.
- Campana, S., 1999. Chemistry and composition of fish otoliths: pathways, mechanisms and applications. *Mar. Ecol. Prog. Ser.* 188 (00), 263–297. <https://doi.org/10.3354/meps188263>.
- Campana, S.E., Thorrold, S.R., 2001. Otoliths, increments, and elements: Keys to a comprehensive understanding of fish populations? *Can. J. Fish. Aquat. Sci.* 58 (1), 30–38. <https://doi.org/10.1139/f00-177>.
- Casselman, J., 1995. Age, growth and environmental requirements of pike, 1st Ed. Springer, Dordrecht, pp. 69–101. <https://doi.org/10.1007/978-94-015-8775-4>.
- Chung, M.T., Jørgensen, K.E.M., Trueman, C.N., Knutsen, H., Jorde, P.E., Grønkvær, P., 2020. First measurements of field metabolic rate in wild juvenile fishes show strong

- thermal sensitivity but variations between sympatric ecotypes. *Oikos* 130 (2), 287–299. <https://doi.org/10.1111/oik.07647>.
- Dahlke, F.T., Wohlrab, S., Butzin, M., Pörtner, H.-O., 2020. Thermal bottlenecks in the life cycle define climate vulnerability of fish. *Science* 369 (6499), 65–70. <https://doi.org/10.1126/science.aaz3658>.
- Darnaude, A.M., Hunter, E., 2018. Validation of otolith  $\delta^{18}\text{O}$  values as effective natural tags for shelf-scale geolocation of migrating fish. *Mar. Ecol. Prog. Ser.* 598 (00), 167–185. <https://doi.org/10.3354/meps12302>.
- Degens, E.T., Deuser, W.G., Haedrich, R.L., 1969. Molecular structure and composition of fish otoliths. *Mar. Biol.* 2 (2), 105–113. <https://doi.org/10.1007/bf00347005>.
- Dhellemmes, F., Rittweg, T., Wiedenbeck, M., Fietzke, J., Trueman, J., Arlinghaus, R., 2023. Hechtökotypen nach Verhalten und Habitatwahl. In Arlinghaus et al. (2023) *BODDENHECHT – Ökologie, Nutzung und Schutz von Hechten in den Küstengewässern Mecklenburg-Vorpommerns. Berichte des IGB* 33.
- Geffen, A.J., 2012. Otolith oxygen and carbon stable isotopes in wild and laboratory-reared plaice (*Pleuronectes platessa*). *Environ. Biol. Fishes* 95 (4), 419–430. <https://doi.org/10.1007/s10641-012-0033-2>.
- Guiguer, K.R.R.A., Drimmie, R., Power, M., 2003. Validating methods for measuring  $\delta^{18}\text{O}$  and  $\delta^{13}\text{C}$  in otoliths from freshwater fish. *Rapid Commun. Mass Spectrom.* 17 (5), 463–471. <https://doi.org/10.1002/rcm.935>.
- Hane, Y., Kimura, S., Yokoyama, Y., Miyairi, Y., Ushikubo, T., Ishimura, T., Nishida, K., 2020. Reconstruction of temperature experienced by Pacific bluefin tuna *Thunnus orientalis* larvae using SIMS and microvolume CF-IRMS otolith oxygen isotope analyses. *Mar. Ecol. Prog. Ser.* 649 (00), 175–188. <https://doi.org/10.3354/meps13451>.
- Hane, Y., Ushikubo, T., Yokoyama, Y., Miyairi, Y., Kimura, S., 2022. Natal origin of Pacific bluefin tuna *Thunnus orientalis* determined by SIMS oxygen isotope analysis of otoliths. *PLoS ONE* 17 (8), 21. <https://doi.org/10.1371/journal.pone.0272850>.
- Heidemann, F., Marohn, L., Hinrichsen, H., Huwer, B., Hüsey, K., Klügel, A., Hanel, R., 2012. Suitability of otolith microchemistry for stock separation of Baltic cod. *Mar. Ecol. Prog. Ser.* 465 (00), 217–226. <https://doi.org/10.3354/meps09922>.
- Helser, T., Kestelle, C., Crowell, A., Ushikubo, T., Orland, I.J., Kozdon, R., Valley, J.W., 2018. A 200-year archaeozoological record of Pacific cod (*Gadus macrocephalus*) life history as revealed through ion microprobe oxygen isotope ratios in otoliths. *J. Archaeol. Sci. -Rep.* 21 (00), 1236–1246. <https://doi.org/10.1016/j.jasrep.2017.06.037>.
- Horton, T.W., Defliese, W.F., Tripathi, A., Oze, C., 2015. Evaporation induced  $^{18}\text{O}$  and  $^{13}\text{C}$  enrichment in lake systems: A global perspective on hydrologic balance effects. *Quat. Sci. Rev.* 131 (B), 1–15. <https://doi.org/10.1016/j.quascirev.2015.06.030>.
- Hüsey, K., Mosegaard, H., Jessen, F., 2004. Effect of age and temperature on amino acid composition and the content of different protein types of juvenile Atlantic cod (*Gadus morhua*) otoliths. *Can. J. Fish. Aquat. Sci.* 61 (6), 1012–1020. <https://doi.org/10.1139/f04-037>.
- Kafemann, R., Adlerstein, S., Neukamm, R., 2000. Variation in otolith strontium and calcium ratios as an indicator of life-history strategies of freshwater fish species within a brackish water system. *Fisheries Research* 46 (1–3), 313–325. [https://doi.org/10.1016/s0165-7836\(00\)00156-9](https://doi.org/10.1016/s0165-7836(00)00156-9).
- Kozdon, R., Ushikubo, T., Kita, N.T., Spicuzza, M., Valley, J.W., 2009. Intratest oxygen isotope variability in the planktonic foraminifer *N. pachyderma*: Real vs. apparent vital effects by ion microprobe. *Chem. Geol.* 258 (3–4), 327–337. <https://doi.org/10.1016/j.chemgeo.2008.10.032>.
- Matta, M.E., Orland, I.J., Ushikubo, T., Helsel, T.E., Black, B.A., Valley, J.W., 2013. Otolith oxygen isotopes measured by high-precision secondary ion mass spectrometry reflect life history of a yellowfin sole (*Limanda aspera*). *Rapid Commun. Mass Spectrom.* 27 (6), 691–699. <https://doi.org/10.1002/rcm.6502>.
- Morales-Nin, B.Y.O., 1986. Structure and composition of otoliths of Cape hake *Merluccius capensis*. *South Afr. J. Mar. Sci.* 4 (1), 3–10. <https://doi.org/10.2989/025776186784461639>.
- Morisette, O., Bernatchez, L., Wiedenbeck, M., Sirois, P., 2020. Deciphering lifelong thermal niche using otolith  $\delta^{18}\text{O}$  thermometry within supplemented lake trout (*Salvelinus namaycush*) populations. *Freshw. Biol.* 65 (6), 1114–1127. <https://doi.org/10.1111/fwb.13497>.
- Nordahl, O., Koch-Schmidt, P., Tibblin, P., Forsman, A., Larsson, P., 2019. Vertical movements of coastal pike (*Esox lucius*)—on the role of sun basking. *Ecol. Freshw. Fish.* 29, 18–30. <https://doi.org/10.1111/eff.12484>.
- Oehler, D.Z., Robert, F., Walter, M.R., Sugitani, K., Allwood, A., Meibom, A., Gibson, E. K., 2009. NanoSIMS: Insights to biogenicity and syngeneity of archaean carbonaceous structures. *Precambrian Res.* 173 (1), 70–78. <https://doi.org/10.1016/j.precamres.2009.01.001>.
- Oehlerich, M., Baumer, M., Lücke, A., Mayr, C., 2013. Effects of organic matter on carbonate stable isotope ratios ( $\delta^{13}\text{C}$ ,  $\delta^{18}\text{O}$  values)—implications for analyses of bulk sediments. *Rapid Commun. Mass Spectrom.* 27 (6), 707–712. <https://doi.org/10.1002/rcm.6492>.
- Pagel, T., Bekkevold, D., Pohlmeier, S., Wolter, C., Arlinghaus, R., 2015. Thermal and maternal environments shape the value of early hatching in a natural population of a strongly cannibalistic freshwater fish. *Oecologia* 178 (4), 951–965. <https://doi.org/10.1007/s00442-015-3301-y>.
- Patterson, W.P., Smith, G.R., Lohmann, K.C., 1993. Continental paleothermometry and seasonality using the isotopic composition of aragonitic otoliths of freshwater fishes. *Geophys. Monogr. Ser.* 78, 191–202.
- Pursiainen, A., Veneranta, L., Kuningas, S., Saarinen, A., Kallavuo, M., 2021. The more sheltered, the better – coastal bays and lagoons are important reproduction habitats for pike in the northern Baltic Sea. *Estuar., Coast. Shelf Sci.* 259, 107477. <https://doi.org/10.1016/j.ecss.2021.107477>.
- Reis-Santos, P., Gillanders, B.M., Sturrock, A.M., Izzo, C., Oxman, D.S., Lueders-Dumont, J.A., Walther, B.D., 2022. Reading the biomineralized book of life: expanding otolith biogeochemical research and applications for fisheries and ecosystem-based management. *Rev. Fish. Biol. Fish.* 33 (2), 411–449. <https://doi.org/10.1007/s11160-022-09720-z>.
- Rittweg, T.D., Trueman, C., Ehrlich, E., Wiedenbeck, M., Arlinghaus, R., 2023. Corroborating otolith age using oxygen isotopes and comparing outcomes to scale age: Consequences for estimation of growth and reference points in northern pike (*Esox lucius*). *Fish. Manag. Ecol.* 31 (1), e12646. <https://doi.org/10.1111/fme.12646>.
- Rittweg, T.D., Trueman, C., Wiedenbeck, M., Fietzke, J., Wolter, C., Talluto, L., Dennenmoser, S., Nolte, A., Arlinghaus, R., 2024. Variable habitat use supports fine-scale population differentiation of a freshwater piscivore (northern pike, *Esox lucius*) along salinity gradients in brackish lagoons. *Oecologia* 00 (0), 1–18. <https://doi.org/10.1007/s00442-024-05627-7>.
- Sunde, J., Yıldırım, Y., Tibblin, P., Bekkevold, D., Skov, C., Nordahl, O., Larsson, P., Forsman, A., 2022. Drivers of neutral and adaptive differentiation in pike (*Esox lucius*) populations from contrasting environments. *Mol. Ecol.* 31 (4), 1093–1110. <https://doi.org/10.1111/mec.16315>.
- Stevenson, D.K., Campana, S.E., 1992. Otolith microstructure examination and analysis. Department of Fisheries and Oceans, Ottawa.
- von Bertalanffy, L., 1938. A quantitative theory of organic growth (inquiries on growth laws. II). *Hum. Biol.* 10 (2), 181–213. (<https://www.jstor.org/stable/41447359>).
- Werner, E.E. (1988). Size, Scaling, and the Evolution of Complex Life Cycles. *Size-Structured Populations: Ecology and Evolution*, Berlin, Heidelberg, 60–81.
- Wycech, J.B., Kelly, D.C., Kozdon, R., Orland, I.J., Spero, H.J., Valley, J.W., 2018. Comparison of  $\delta^{18}\text{O}$  analyses on individual planktic foraminifer (*Orbulina universa*) shells by SIMS and gas-source mass spectrometry. *Chem. Geol.* 483 (00), 119–130. <https://doi.org/10.1016/j.chemgeo.2018.02.028>.